

Infrared Dichroism and Birefringence Studies of Silica-Filled Styrene–Butadiene Rubbers

L. BOKOBZA,¹ L. LADOUCE,² Y. BOMAL,² B. AMRAM²

¹ Laboratoire de Physico-Chimie Structurale et Macromoléculaire, ESPCI, 10 rue Vauquelin, 75231 Paris, Cedex 05, France

² Rhodia, Centre de Recherches d'Aubervilliers, 52 rue de la Haie Coq, 93308 Aubervilliers Cedex, France

Received 27 September 2000; accepted 24 December 2000

ABSTRACT: Infrared and birefringence measurements are used to characterize the orientational behavior of silica-filled styrene–butadiene copolymers. The orientational data are correlated with the results of equilibrium swelling measurements. On the other hand, the role played by a silane coupling agent bis(3-triethoxysilylpropyl)tetrasulfide (TESPT), or “Si69” on rubber/silica system is discussed. © 2001 John Wiley & Sons, Inc. *J Appl Polym Sci* 82: 1006–1012, 2001

Key words: styrene–butadiene copolymers; elastomers; reinforcement; silica; silane coupling agent; swelling measurements; orientation; infrared dichroism; near-infrared spectroscopy; birefringence

INTRODUCTION

The commercial applications of elastomers often require the use of particulate fillers to obtain the desired reinforcement. In the rubber industry, besides carbon black, silica is the other reinforcing filler used to impart specific properties to rubber compounds.¹ The use of silicas in combination with bifunctional coupling agents is becoming important in rubber applications.^{2,3}

Coupling agents are generally bifunctional molecules that are able to establish molecular bridges at the interface between the polymer matrix and the filler surface. In this way, the rubber-filler adhesion is increased, and consequently, the reinforcing capability of silica is enhanced. One of the most effective coupling agent for sulfur cured compounds filled with nonblack fillers is mercaptopyltrimethoxysilane (Dynasilan). The bis(3-tri-

ethoxysilylpropyl)-tetrasulfide (TESPT), commonly abbreviated “Si69” has widened the use of silica in rubber applications. It is often mentioned that the tetrasulfane function of the “Si69” reacts with the polymer under curing conditions, thus leading to an additional network crosslinking, rather than interfacial coupling.⁴

This article describes investigations that were carried out with state-of-the-art techniques: infrared dichroism and birefringence, able to bring information at a molecular level. In addition, swelling measurements are also carried out in order to get an indirect estimation of the crosslink density of the networks.

The aim of the study is to investigate the effect of Si69 on (1) the cure characteristics of styrene–butadiene rubbers, and (2) the orientational behavior of silica-filled styrene–butadiene vulcanizates.

EXPERIMENTAL

Samples

All the samples were obtained from a solution of styrene–butadiene rubber (VSL 5525-1 from

Correspondence to: L. Bokobza (liliane.bokobza@espci.fr).

Journal of Applied Polymer Science, Vol. 82, 1006–1012 (2001)
© 2001 John Wiley & Sons, Inc.

Table I Formulations of the Rubber Compounds

Ingredients (phr)	M1	M2	M3	M4	M5
Rubber	100	100	100	100	100
Silica (150 m ² /g)	0	58	58	0	0
Si69	0	0	4.64	4.64	4.64
Sulfur	1.1	1.1	1.1	1.1	0
Diphenyl guanidine (DPG)	1.45	1.45	1.45	1.45	1.45
Zinc oxide	1.82	1.82	1.82	1.82	1.82
Stearic acid	1.1	1.1	1.1	1.1	1.1
Cyclohexyl benzothiazole sulfenamide (CBS)	1.3	1.3	1.3	1.3	1.3

Bayer) that contains 25 wt % of the styrene units. The microstructure of the butadiene phase is as follows: 10% *cis*, 17% *trans*, 73% 1,2. On the other hand, 27 wt % of oil is added to the polymer.

The formulation and the vulcanization characteristics of the samples are compiled in Table I.

Methods of Investigation

All experiments reported here were performed at room temperature.

To determine the equilibrium swelling of the vulcanizate, a sample of 20 × 10 × 0.2 mm was put into toluene. After 72 h at room temperature, the sample was taken out of the liquid, the toluene removed from the surface, and the weight determined for the swollen compound and for the dried sample (without oil). The equilibrium swelling ratio, Q (volume of the network plus solvent/volume of the dry network), was also determined from the lengths of the sample in the unswollen and swollen states.

Infrared spectra were recorded with a Magna-IR 560 FTIR spectrometer equipped with a high-energy Ever-Glo source, a XT-KBr beamsplitter for spectral range coverage from 11,000 to 375 cm⁻¹ and a MCT detector. The spectra were recorded with a resolution of 4 cm⁻¹ and an accumulation of 32 scans.

Birefringence was measured by using an Olympus BHA polarizing microscope fitted with a Berrek compensator. The thickness of the sample was obtained with a micrometer comparator and averaged all along the specimen.

THEORETICAL BACKGROUND

Infrared Dichroism Measurements

The absorption of infrared radiation is caused by the interaction of the electric field vector of the

incident light with the electric dipole-transition moment associated with a particular molecular vibration:

$$A \propto (\vec{M} \cdot \vec{E})^2 \quad (1)$$

Segmental orientation in a network subjected to uniaxial elongation may be conveniently described by the second Legendre polynomial:⁵

$$\langle P_2(\cos \theta) \rangle = (3\langle \cos^2 \theta \rangle - 1)/2 \quad (2)$$

where θ is the angle between the macroscopic reference axis (usually taken as the direction of strain) and the local chain axis of the polymer. The angular brackets indicate an average over all molecular chains and over all possible configurations of these chains.

The effect of anisotropy on a selected absorption band of the infrared spectrum of the sample is reflected by the dichroic ratio R , defined as $R = A_{//}/A_{\perp}$ ($A_{//}$ and A_{\perp} being the absorbances of the investigated band, measured with radiation polarized parallel and perpendicular to the stretching direction, respectively).

The orientation function $\langle P_2(\cos \theta) \rangle$ is related to the dichroic ratio R by the expression:

$$\begin{aligned} \langle P_2(\cos \theta) \rangle &= \frac{2}{(3 \cos^2 \beta - 1)} \cdot \frac{(R - 1)}{(R + 2)} \\ &= \mathbf{F}(\beta) \frac{(R - 1)}{(R + 2)} \quad (3) \end{aligned}$$

where $\mathbf{F}(\beta)$ only depends on the angle β between the transition moment vector of the vibrational mode considered and the local chain axis of the polymer or any directional vector characteristic of a given chain segment (Fig. 1).

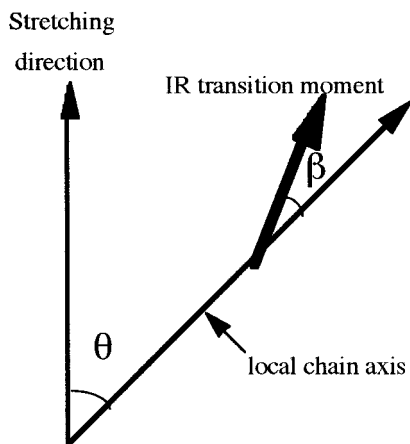


Figure 1 Positions of local chain axis and transition moment with respect to the stretching direction.

One can express the orientation of the transition moment vector, $\langle P_2(\cos \gamma) \rangle$, with respect to the direction of stretch, by the following expression:

$$\langle P_2(\cos \gamma) \rangle = \frac{R - 1}{R + 2} \quad (4)$$

The orientation function that characterizes the segmental orientation in an affine network model under uniaxial extension is given by the following expression:^{6–8}

$$\langle P_2(\cos \theta) \rangle_{\text{affine}} = D_0(\alpha^2 - \alpha^{-1}) \quad (5)$$

where α is the extension ratio defined as the ratio of the final length of the sample in the direction of stretch to the initial length before deformation, and D_0 is the configurational factor. This factor, which incorporates the structural features of the network chains, only reflects the intrinsic orientational behavior of a single chain that is not subject to any orientational correlations with the spatially neighboring chains. This configurational factor, which represents the “orientability” of the chain segments, can be estimated by the rotational isomeric state approach.⁹ Let us mention that in the other extreme case of phantomlike chains, the orientation function becomes:^{10,11}

$$\langle P_2(\cos \theta) \rangle_{\text{phantom}} = D_0(1 - 2/\phi)(\alpha^2 - \alpha^{-1}) \quad (6)$$

where ϕ is the functionality of the junctions.

The analysis of the orientational behavior of filled networks can provide a direct estimation of the total network chain density because D_0 is

inversely proportional to the number n of bonds in the chain between two junctions.

Infrared measurements can be performed either in the mid- or in the near-infrared range.

One practical problem in the case of infrared dichroism measurements arises from the requirement of band absorbance, which should be roughly lower than 0.7 to permit use of the Beer-Lambert law, although absorbances appreciably higher can be used with great care. That implies use of sufficiently thin films. Depending on the extinction coefficient of the considered band, the required thickness can range from 1 to 200 μm . From this point of view, polymers with strong absorption bands are difficult to study. This difficulty can now be overcome by using near-infrared (NIR) spectroscopy, which examines overtones and combination bands much weaker than the fundamental modes.

The NIR region of the spectrum covers the interval from about 12,500–4000 cm^{-1} (800–2500 nm). The bands in the NIR are primarily overtones and combinations of the fundamental absorbances found in the classical mid-IR region. The absorption bands appearing in the NIR range arise from overtones and combinations of fundamental vibrations of hydrogen-containing groups such as C—H, N—H, and O—H. As these bands are much weaker than the corresponding fundamental absorptions, a NIR spectrum is considerably simplified compared to the usual mid-IR region. Consequently, the principal advantage of NIR analysis is the ability to examine specimens several mm thick. In other words, the NIR region, which complements the mid-IR region, is analytically useful for spectroscopic applications involving analysis of samples containing very strong mid-IR absorbers.¹²

Another problem occurring in the mid-infrared spectra of crosslinked rubbers arises from some absorptions of the formulation ingredients listed in Table I. These absorptions, which “spoil” the mid-infrared spectra, vanish in the near-infrared region. Consequently, measurements carried out in the near-infrared spectra of the samples are more accurate than those obtained in the mid-infrared range.

Birefringence

Measurements of strain birefringence of deformed networks is an alternative technique for determining the degree of orientation of chain segments.^{13,14}

According to the theory, in an affine network model, the birefringence is related to the strain function by the expression:

$$\Delta n = \frac{\nu k T C}{V} (\alpha^2 - \alpha^{-1}) = D_1 (\alpha^2 - \alpha^{-1}) \quad (7)$$

where ν/V represents the number of chains per unit volume, and C is the stress-optical coefficient that is related to the optical anisotropy Γ_2 of the network through the following equation:

$$C = \frac{2\pi(n^2 + 2)^2\Gamma_2}{27nkT} \quad (8)$$

n being the mean refractive index. C is usually referred to in the literature as the stress-optical coefficient, because:

$$C = \Delta n / \sigma \quad (9)$$

where σ is the true stress (force f divided by the deformed area A) given in the affine network model by:

$$\sigma = \frac{\nu k T}{V} (\alpha^2 - \alpha^{-1}) \quad (10)$$

The relation between birefringence and the second-order moment of the orientation function is given by the expression:

$$[\Delta n] = [\Delta n]_0 \langle P_2(\cos \theta) \rangle \quad (11)$$

where $[\Delta n]_0$ is the intrinsic birefringence characteristic of the polymer.

$[\Delta n]_0$ may be called the maximum birefringence because the perfect orientation corresponds to $\langle P_2(\cos \theta) \rangle = 1$.

Swelling Measurements

The average chain length M_c can be estimated from swelling measurements by using the following equation:

$$M_c = - \frac{\rho(1 - 2/\phi)V_1 v_{2m}^{1/3}}{\ln(1 - v_{2m}) + \chi v_{2m}^2 + v_{2m}} \quad (12)$$

In this expression close to the well-known Flory-Rehner equation¹⁵ based on the affine network model, ρ denotes the network density during for-

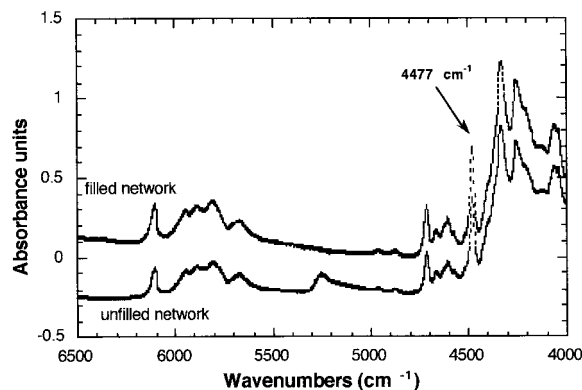


Figure 2 Near-infrared spectra of unfilled (M1) and a filled (M3) networks.

mation, V_1 is the molar volume of solvent, v_{2m} is the volume fraction of polymer at conditions of equilibrium and χ is the interaction parameter for the solvent-polymer system. The front factor $(1 - 2/\phi)$ comes from the fact that at high degree of swelling Q (equal to v_{2m}^{-1}), the system may be treated essentially as a phantom network.

RESULTS AND DISCUSSION

Infrared Dichroism and Birefringence Measurements

As a typical example, the near-infrared spectra of the unfilled (M1) and a filled (M3) samples are represented in Figure 2 between 4000 and 6500 cm^{-1} .

We have examined the dichroic behavior of the band located at 4477 cm^{-1} ascribed to a combination of a stretching and a bending mode of the vinyl group. This band, being associated with a particular functional group of the polymer, will consequently reflect the orientational behavior of the macromolecular chains.

Effect of Silica under the Presence of the Silane Coupling Agent Si69

Figure 3 displays the dichroic functions of this band against the strain function $(\alpha^2 - \alpha^{-1})$ for the unfilled sample and for the sample filled with silanized silica. According to eq. (4), these dichroic functions given by the experimental quantity $(R - 1)/(R + 2)$ represent the orientation $\langle P_2(\cos \gamma) \rangle$ of the transition moment vector associated with the band at 4477 cm^{-1} relative to the direction of stretch. This way of plotting the data precludes

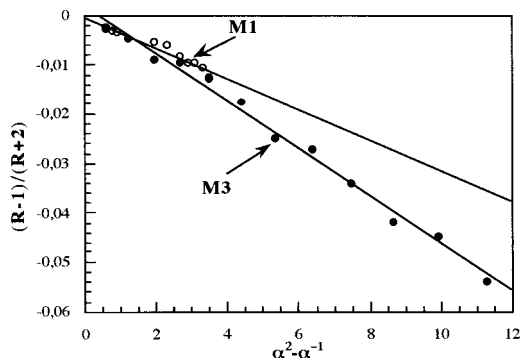


Figure 3 Dichroic functions for the band at 4477 cm^{-1} .

any assumption concerning the local chain axis, which is a rather fictitious entity, defined as an axis of cylindrical symmetry with respect to the transition moment vector. It is worthwhile to notice that, in practice, in data interpretation, the orientation of the local chain axis is determined rather than the orientation of specific transition moments. But, in this work, as long as we are looking at the dichroic behavior of the same absorption band, we can consider that $\langle P_2(\cos\theta) \rangle$ is proportional to the dichroic function.

As seen in Figure 3, the 4477 cm^{-1} exhibits a negative orientation (negative D_0 or $\langle P_2(\cos\gamma) \rangle$), thus proving that the corresponding transition moment is most likely perpendicular to the local chain axis.

Figure 4 shows for the M1 and M3 samples, the birefringence as a function of $(\alpha^2 - \alpha^{-1})$. Following the practice, we can determine the stress-optical coefficient C by plotting birefringence against the true stress. The results displayed in Figure 5 are related to the unfilled sample.

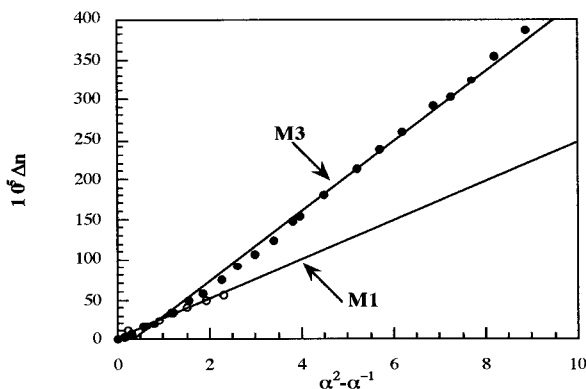


Figure 4 Strain dependence of the birefringence.

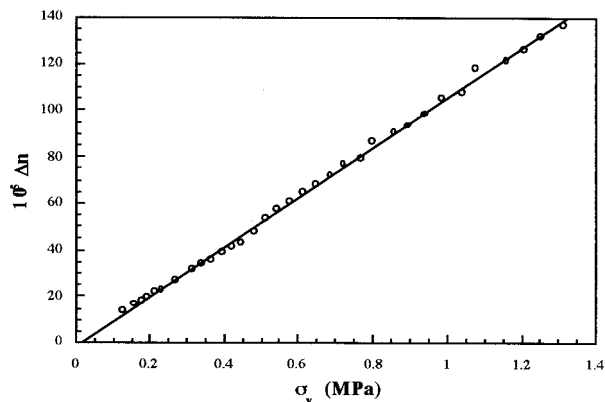


Figure 5 Determination of the stress-optical coefficient for the unfilled sample.

If, we plot, for the filled sample (M3) the birefringence against stress, we get a nonlinear relationship, the increase in stress being larger at high deformation (Fig. 6).

The observed differences between stress and orientation in filled networks result from finite chain extensibility. Especially at higher degrees of reinforcement, the presence of short chains connecting filler particles contributes to the modulus significantly, and at the limit of maximum extensibility, no further orientation of segments is possible.¹⁶

The higher molecular order obtained by addition of silica in the presence of the coupling agent (Si69) is attributed to filler-rubber interactions leading to an introduction of additional crosslinks into the network by the filler.

Effect of Silica in the Absence of a Coupling Agent

When silica is added in the medium in the absence of a coupling agent (M2 sample), we observe

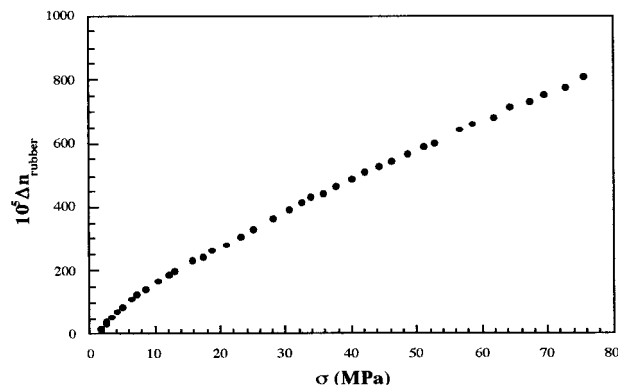


Figure 6 Birefringence against stress for the M3 sample.

a decrease in the overall network chain density reflected by a decrease in the configurational factor D_0 and a decrease in the slope of the curve D_1 representing the birefringence against the strain function (Table II). This effect already observed in the case of silica-filled natural rubber is attributed to the interaction of the silica with the chemical ingredients of the formulation, thus removing them from the vulcanization reaction and inhibiting proper crosslink formation.¹⁷

Influence of Si69 on the Curing Characteristics

It is generally admitted that the coupling reaction of Si69 can be divided into two separate steps. First, the ethoxy groups of Si69 react with the silanols groups on the silica surface, then the tetrasulfane function is split and reacts with the rubber chains under curing conditions by forming filler rubber bonds.¹⁸

To investigate the cocuring effect of Si69, we have investigated the orientational properties of two different networks. Both of them are cured under the presence of the silane coupling agent, but in the first case, in the absence of silica (M4) and in the second case, in the absence of silica and sulfur (M5).

As shown in Table II, in the absence of silica, the coupling agent does not seem to have a significant effect on the vulcanization process. The resultant network has, within the experimental accuracy, the same orientational properties as those of the unfilled network (M1).

In the absence of the vulcanizing agent, a crosslinking reaction can also take place, but leads to a looser network. This fact has already been reported where polymer gelation was observed when a gum compound containing only gel-free solution SBR, zinc oxide, stearic acid, and antioxidant was heated at 160°C.¹⁹

Table II Swelling and Orientational Characteristics of the Rubber Compounds

Samples	Rubber Equilibrium Swelling Ratios	$10^3 D_0$	$10^5 D_1$
M1	6.84	-3.2	24.7
M2	7.17	-2.7	22.7
M3	4.31	-4.8	43.6
M4	6.30	-3.3	25.8
M5	8.22	-1.1	15.9

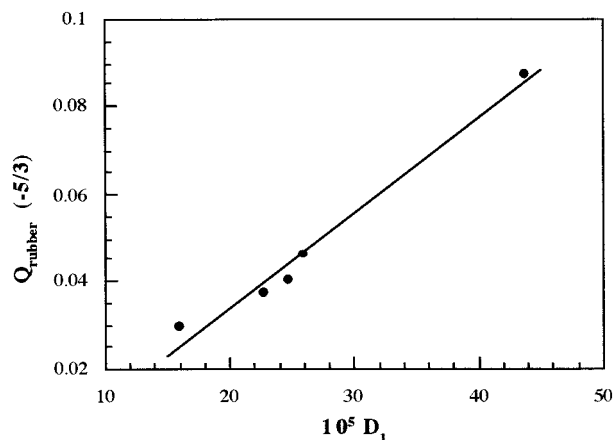


Figure 7 Correlation between equilibrium swelling and birefringence measurements.

Correlation between the Swelling and Orientational Measurements

The swelling measurements at equilibrium can be correlated to the orientation data; both measurements are sensitive to the apparent molecular weight between crosslinks.

It has to be mentioned that under the assumption that the filler does not swell, we can calculate the equilibrium swelling ratio of the rubber alone, which is equal to:

$$Q_{\text{rubber}} = \frac{Q - \phi}{1 - \phi} \quad (13)$$

where ϕ is the volume fraction of filler.

On the other hand, at high degrees of swelling, a series expansion of eq. (12) leads to the following expression:

$$(1/M_c) \propto v_2^{5/3} = Q_{\text{rubber}}^{-5/3} \quad (14)$$

The configurational factor (D_0) as well as the slope of the curve D_1 representing the birefringence against the strain function have been shown to be proportional to $1/M_c$.

The nice correlation obtained between the swelling measurements and the orientation data (taken from birefringence measurements in Fig. 7) for all the investigated samples, validates the consistency of this new approach.

CONCLUSIONS

This article has described recent investigations on styrene-butadiene copolymers carried out by

techniques based on measurements of chain orientation. It is shown that the use of silica in combination of the bifunctional organosilane leads of an increase in the crosslinking density of the elastomeric network. In the absence of silica, Si69 does not seem to affect the orientational properties of the elastomeric network.

REFERENCES

1. Wagner, M. P. *Rubber Chem Technol* 1976, 49, 703.
2. Wolff, S. *Rubber Chem Technol* 1996, 69, 325.
3. Gelling, I. R.; Porter, M. *Natural Rubber Science and Technology*; Eirich, F. R., Ed.; Academic Press: New York, 1978; p. 367.
4. Hashim, A. S.; Azahari, B.; Ikeda, Y.; Kohjiya, S. *Rubber Chem Technol* 1998, 71, 289.
5. Jasse, B.; Koenig, J. L. *J Macromol Sci Rev Macromol Chem* 1979, C17, 61.
6. Nagay, K. *J Chem Phys* 1964, 40, 2818.
7. Roe, R. J.; Krigbaum, W. R. *J Appl Phys* 1964, 35, 2215.
8. Erman, B.; Haliloglu, T.; Bahar, I.; Mark, J. E. *Macromolecules* 1991, 24, 901.
9. Besbes, S.; Cermelli, I.; Bokobza, L.; Monnerie, L.; Bahar, I.; Erman, B.; Herz, J. *Macromolecules* 1992, 25, 1949.
10. Mark, J. E.; Erman, B. *Rubber Elasticity. A Molecular Primer*; Wiley-Interscience: New York, 1988.
11. Erman, B.; Mark, J. E. *Structure and Properties of Rubberlike Networks*; Oxford University Press: New York, 1997.
12. Bokobza, L. *J Near Infrared Spectrosc* 1998, 6, 3.
13. Erman, B.; Flory, P. J. *Macromolecules* 1983, 16, 1601.
14. Erman, B.; Flory, P. J. *Macromolecules* 1983, 16, 1607.
15. Flory, P. J.; Rehner, J. *J Chem Phys* 1944, 12, 412.
16. Bokobza, L.; Erman, B. *Macromolecules* 2000, 33, 885.
17. Kravlevich, M. L.; Koenig, J. L. *Rubber Chem Technol* 1998, 71, 300.
18. Goerl, U.; Hunsche, A.; Mueller, A.; Koban, H. G. *Rubber Chem Technol* 1997, 70, 608.
19. Wang, M.-J. *Rubber Chem Technol* 1998, 71, 520.